

## **NUCLEAR LABORATORY SETUP FOR MEASURING THE SOIL WATER CONTENT IN ENGINEERING PHYSICS TEACHING LABORATORIES**

**Dr. Arun balaji R, N. Dattathreya, Dr. Ilaiyakumar I** <sup>2</sup>Assistant Professor, <sup>1,3</sup>professor <sup>1,2</sup>Department of Physics, <sup>3</sup>Department of English Bheema Institute of Technology and Science, Adoni

### **Abstract:**

One important soil parameter that is measured in many engineering, geology, soil and environmental science investigations is the soil water content ( $\theta$ ). For example,  $\theta$  influences the assessment of soil strength, hydraulic conductivity, groundwater recharge, and soil aeration condition. Measurement of  $\theta$  is essential for tracking and managing a number of soil processes. A quick and non-destructive method for determining  $\mu$  in soils with drastically different compositions is the gamma-ray attenuation (GRA) approach. However, lab physics classes rarely cover GRA. An experiment involving the measurement of  $\theta$  using a teaching GRA apparatus is proposed. A Geiger-Müller detector, a radiation counter, and a radioactive source with a  $^{137}\text{Cs}$  decay were the components of the experimental setup. Four different granulometric compositions of soil samples were examined. The transmitted gamma-ray photon intensity and  $\theta$  were found to have strong linear relationships (correlation coefficients ranging from  $-0.95$  to  $-0.98$ ). There were variations in the soil porosity between the traditional and GRA techniques, ranging from around 7.8% to about 18.2%. Furthermore, a robust linear correlation (correlation coefficients ranging from 0.90 to 0.98) was noted between the GRA and the conventional gravimetric technique for measuring  $\theta$ . The effectiveness of the teaching GRA apparatus in measuring  $\theta$  was confirmed. Additionally, the device enables undergraduate students from a variety of subject areas to be introduced to a few significant facets of the study of contemporary physics.

**Keywords:** attenuation coefficient, soil granulometry, soil porosity,  $^{137}\text{Cs}$  gamma-ray photons, and soil aggregates.

### **1 . Introduction**

Water is an essential element for life. For plants, it is stored and retained by capillarity in the pores of the soil skeleton [1]. The soil water content ( $\theta$ ), which can be expressed in terms of mass or volume percentages, is a measure that often is related to the maintenance and establishment of irrigated crops. Rational water usage in agriculture is an issue of great relevance since it consumes 70% of all the freshwater used worldwide [2]. Unfortunately, half of this consumed water is wasted due to inappropriate usage in different agricultural practices developed all around the world. In addition, to be absorbed, the water present in the soil must be available to the plant [3].

Soil is considered saturated when its entire pore space is filled with water [4]. In opposition, the soil is dry when all its pore space is filled with air. Between these two extremes, the soil is said to be moist. According to the existing literature, there are different methodologies for determining  $\theta$  [1]. The standard (traditional) method is based on the determination of the mass or volume of water present in the sample at the time it is analyzed [5]. Other methods for measuring  $\theta$  are based on the interaction of photons or particles with the sample. Among them, there are methods based on the moderation of fast neutrons or the attenuation of gamma radiation [6]. Soil water content analysis can be accomplished by investigating laboratory samples or under field conditions, depending on the study carried out.

In undergraduate courses in applied physics to engineering, the concept of soil water content is fundamental for determining the physical-hydric behavior of the soil [7,8]. Additionally,  $\theta$  determination is fundamental for the evaluation of the soil water retention curve and hydraulic conductivity [9–11]. Equipment based on the interaction of radiation with the matter for measuring  $\theta$  is rarely available to engineering undergraduate students. In general, these types of equipment are found in institutions that develop research related to applied nuclear techniques and are restricted to graduate research activities [12–16].

This study presents the use of a simplified gamma-ray attenuation (GRA) system, developed for teaching purposes, as an alternative to the traditional GRA systems usually employed in soil properties analyses [6,10,12–16]. The simplified system consists of a Geiger-Müller detector, low-activity radioactive sources, and a photon counting system. To the best of our knowledge, there are no articles exploring GRA systems for  $\theta$  measurements aimed at undergraduate engineering students. Thus, our study proposes a procedure for monitoring  $\theta$  in soil samples under different moisture conditions using a simplified GRA system. Moreover, the suggested approach presents a detailed description of the theoretical aspects of the measurements, which can guide professors in conducting teaching activities involving this knowledge.

The results obtained and presented here indicate that the proposed approach is quite adequate in determining the  $\theta$  of soil samples of contrasting textures (granulometries). However, this study is not intended to replace the existing traditional GRA systems. Our approach just consists of a good alternative for teaching activities, in which the concepts of soil water content, soil pore space, radiation interaction with matter, and radiation production and detection can be satisfactorily explored.

## 2. Basic Theory

Beer-Lambert's law is used for describing the gamma-ray attenuation by any material, including soil samples. Soil is a three-phase system composed of solids (minerals and organic materials), solutes (water), and gases (air) (Figure 1a). For a collimated beam of gamma-rays interacting with the soil, Beer-Lambert's law is written as follows [13]:

$$I = I_0 e^{-(\mu_{pp} \rho_p x + \mu_{wp} \rho_w x + \mu_{ap} \rho_a x)} \quad (1)$$

where  $I_0$  (cps: counts per second) is the intensity of the incident beam,  $I$  (cps) is the beam intensity transmitted through the sample (Figure 1b),  $\mu$  ( $\text{cm}^2 \text{g}^{-1}$ ) is the mass attenuation coefficient,  $\rho$  ( $\text{g cm}^{-3}$ ) is the sample density, and  $x$  (cm) is the sample thickness. The subscripts p, w, and a refer to particles, water, and air, respectively.

Frequently, the interaction of the gamma-rays with the air is usually ignored as the air density and its mass attenuation coefficient are much smaller than the density and mass attenuation coefficient of the solids and water. Thus, Equation (1) can be simplified to:

$$I = I_0 e^{-(\mu_{pp} \rho_p x + \mu_{wp} \rho_w x)} \quad (2)$$

As it is known, the soil water content can be measured based on its gravimetric ( $G$ :  $\text{g g}^{-1}$ ) or volumetric ( $\theta$ :  $\text{cm}^3 \text{cm}^{-3}$ ) content [5]. The gravimetric water content represents the water mass ( $m_w$ : g) per unit of dry soil mass ( $m_s$ : g) (Equation (3)), while the volumetric water content is given by the water volume ( $V_w$ :  $\text{cm}^3$ ) per unit of soil volume ( $V_s$ :  $\text{cm}^3$ ) (Equation (4)), usually expressed as a percentage [4]:

$$G = \frac{m_w}{m_s} \quad (3)$$

$$\theta = \frac{V_w}{V_s} = \frac{\rho_s G}{\rho_w} \quad (4)$$

where  $\rho_s$  ( $\text{g cm}^{-3}$ ) is the soil bulk density.

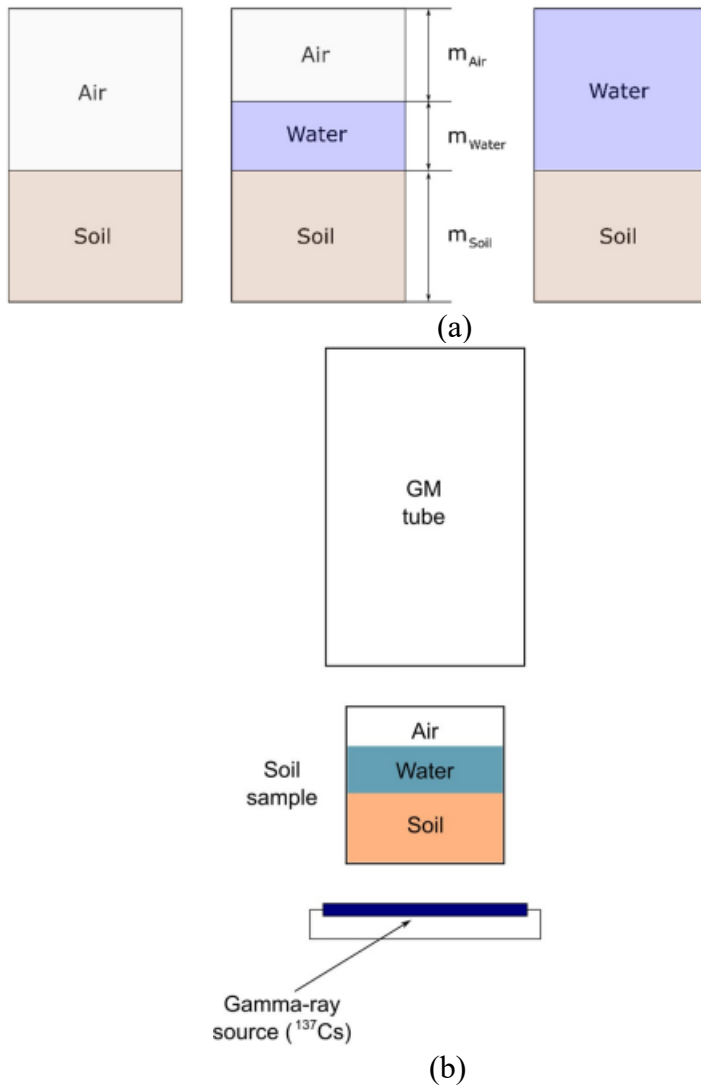


Figure 1. Schematic drawing showing (a) the soil as a three-phase system and (b) the experimental gamma-ray attenuation geometry (the figure is only schematic and not to scale). GM: Geiger-Müller detector. The symbol  $m$  stands for mass.

Based on the concepts of soil bulk and particle densities [1], Equation (2) becomes:

$$I = I_0 e^{-x(\mu_{ps} + \mu_w \theta \rho_w)}. \quad (5)$$

Equation (5) is utilized for measuring, for example, the bulk density when the soil is dry ( $\theta = 0 \text{ cm}^3 \text{ cm}^{-3}$ ) (Figure 1a—left):

$$\rho_s = \frac{1}{x \mu_p} \ln \left( \frac{I_0}{I} \right). \quad (6)$$

If the soil is moist (Figure 1a—center and right), Equation (5) can also be employed for monitoring the sample water content:

$$\theta = \frac{1}{\mu_w \rho_w} \left[ \ln \left( \frac{I_0}{I} \right) - x \mu_p \rho_s \right]. \quad (7)$$

### 3. Materials and Methods

A PASCO kit [17] was used to determine the water content of the investigated soil samples (Figure 2). The setup consists of a  $^{137}\text{Cs}$  radioactive source (reference number SN-7972A), a Geiger-Müller (GM) detector (reference number SN-7970-A), a radiation counter (high voltage source (0 to 1200 V) + timer + counter—reference number SN-7907), a soil sample, and source holders (sample + GM + radioactive source) (see Supplementary Figure S1). The Caesium-137 source

of the kit is a sealed plastic pellet (2.5 cm diameter), whose activity is c. 3.4  $\mu\text{Ci}$ . This radioactive source emits gamma-ray photons with an energy of c. 0.662 MeV. Its half-life is around 30.2 years. According to the manufacturer's specifications, the radioactive source has a stated uncertainty of  $\pm 15\%$ . It is worth mentioning that these radioactive sources are USNRC License Exempt (US) according to the kit manufacturer. In the proposed experiment, three  $^{137}\text{Cs}$  sources were piled (set one above the other) to increase the flux of photons transmitted through the samples. Thus, the total activity of the source assembly was c. 10.2  $\mu\text{Ci}$  [18].

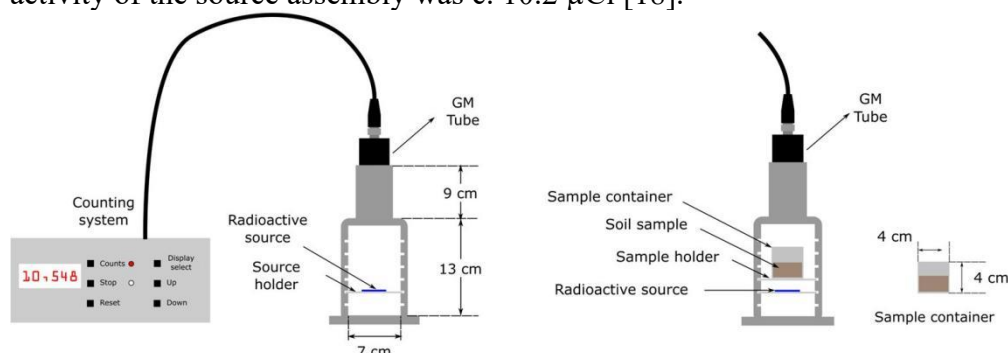


Figure 2. Schematic drawing of the Intermediate Nuclear Laboratory Setup.

The GM detector used in the experiment has a 35-mm diameter window made of mica ( $2 \text{ mg cm}^{-2}$ ) and is designed to enable good counting efficiency for low-activity radioactive sources. The dead time of the tube is around 200  $\mu\text{s}$ . The operating voltage selected to supply the GM was 920 V. A previous experiment was performed to determine the counting plateau of the GM detector, which varied from 760 to 980 V. For the experiment, the radioactive sources and soil samples were placed inside the holder, and since it has slots spaced 1.0 cm apart, the teaching instructor can vary the source and sample positions quickly and easily (Figure 2 and see Supplementary Figure S1).

Due to radiological protection concerns, the classroom instructor is allowed to handle the radioactive sources. However, it is an extra concern, as in this kind of system, the radioactive sources have very low activity. Even to increase this protection, lead plates with a thickness of c. 3 mm can be placed around the radioactive source during the measurements. In these experimental activities, the undergraduate students, placed at a safe distance from the experimental setup (radioactive source + GM detector + sample), only operate the electronics responsible for counting the incident and transmitted gamma-ray photons reaching the GM detector. Additionally, the radioactive source is sealed and has a small window that permits the upward emission of photons perpendicularly to the students' position.

The counts were registered in a radiation counter system (PASCO—Spectech ST-360 Counter) composed of a timer, preset counter, digital ratemeter, computer interface, and battery power for field applications. The interval of time selected for each measurement was 103 s (c. 17 min) (Silt Loam and Heavy Clay soils) and  $5 \times 10^2$  s (c. 8 min) (Sandy Clay Loam and Clay soils). For these time intervals, the obtained uncertainty in the measurements (total counts recorded) was around 1% or less. This time interval was also selected to permit the experimental measurements in two to three classes of 50 min each.

Soil samples with four contrasting particle size fractions, identified as Silt Loam—SiLo, Heavy Clay—HeCa, Sandy Clay Loam—SaCLo, and Clay—Cla, were selected for the experimental measurements (Figure 3). Approximately 100 g of each soil was sieved at 2 mm (10 Mesh). This procedure was performed to produce as much as possible homogeneous soil samples. Before sieving, the soil samples were oven-dried (air-forced circulation) for 24 h at 105  $^{\circ}\text{C}$ .

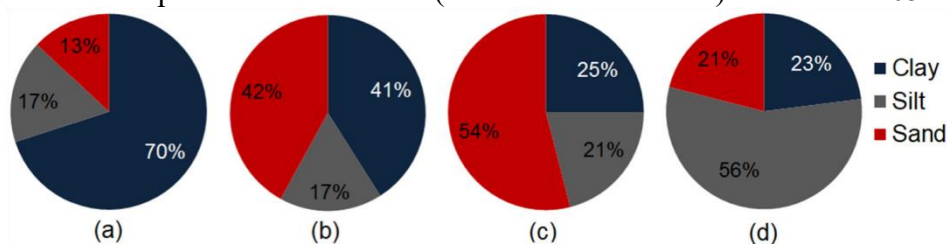


Figure 3. Particle size fractions of the soils studied: (a) Heavy Clay (HeCa), (b) Clay (Cla), (c) Sandy Clay Loam (SaCLo), and (d) Silt Loam (SiLo).

The soil samples were then placed in cylindrical plastic containers with diameters of 3.25 cm and volumes of c. 35 cm<sup>3</sup> (see Supplementary Table S1). Each soil was carefully placed inside the containers for the experiment. To standardize the samples, the sample containers were filled until the sample thickness (soil depth) crossed by the gamma-ray photons from the radioactive source was approximately 2.65 to 2.70 cm (see Supplementary Table S1). This thickness was equivalent to a soil volume of approximately 25 cm<sup>3</sup> inside each container. A pestle with the same container's internal diameter was employed for leveling the soil inside its interior (see Supplementary Figure S1). After filling the container, the soil bulk density of the samples was determined by the gravimetric method (Table 1) [1]:

$$\rho_s = \frac{m_s}{V_s} \quad (8)$$

Table 1. Soil bulk density ( $\rho_s$ ), soil particle density ( $\rho_p$ ), and volume of pores ( $V_{por}$ ) of the contrasting soils studied.

Soil/Properties	$\rho_s$ (g cm <sup>-3</sup> )	$\rho_p$ (g cm <sup>-3</sup> )	$V_{por}$ (cm <sup>3</sup> cm <sup>-3</sup> )
HeCa	1.08	2.63	14.77
Cla	1.20	2.16	11.13
SaCLo	1.10	2.22	12.62
SiLo	1.03	2.25	13.50

HeCa: Heavy Clay; Cla: Clay; SaCLo: Sandy Clay Loam; SiLo: Silt Loam. The soil bulk density was determined using Equation (8), and the volume of pores was determined using Equation (10).

The porosity ( $\phi$ : cm<sup>3</sup> cm<sup>-3</sup>) and volume of pores ( $V_{por}$ : cm<sup>3</sup>) of the soil samples were calculated using Equations (9) and (10), respectively. Afterwards, the samples were moistened by selecting five different  $\theta$  (see Supplementary Table S2). Five different volumes of water were selected ( $V_{por}$  divided by five) to be added, little by little, to the samples. The last volume of water added saturated the sample (Table 1) [5].

$$\phi = 1 - \frac{\rho_s}{\rho_p} \quad (9)$$

$$V_{por} = V_s \phi \quad (10)$$

where the particle density ( $\rho_p$ : g cm<sup>-3</sup>) of the contrasting soils was determined by the gas pycnometer method (see Supplementary Table S1) [19]. In the absence of this measure, in general, the soil particle density is assumed as 2.65 g cm<sup>-3</sup>.

The soil sample (soil + container) under different moisture conditions was placed right above the radioactive source (sealed plastic pellet) to perform the experiments. The volume of water to be added to the soil was controlled using a pipette. The mass measurements were carried out with a precision balance (Gehara AG200, 10<sup>-4</sup> g accuracy). The distance between the radioactive source and the detector was c. 6.5 cm. To prevent the detection of beta particles (energy of c. 0.512 MeV) from the <sup>137</sup>Cs radioactive source, a 0.050 mm thick aluminum plate (supplied by PASCO) was placed between the sample top and the detector window.

Before calculating the soil water content, we measured the photon intensity transmitted through the dry soil samples ( $I$ ) and then the photons transmitted through the moisture soil samples ( $I_\theta$ ) (see Supplementary Table S3). Using Equation (11) the volumetric water content of the sample could be determined as follows:

$$\theta = \frac{1}{\mu_w \rho_w} \ln \frac{I}{I_\theta} \quad (11)$$

The water density value utilized in the calculations was 0.998 g cm<sup>-3</sup>. According to the literature, the water mass attenuation coefficient for photons from <sup>137</sup>Cs is c. 0.0767 cm<sup>2</sup> g<sup>-1</sup> [20].



Figure 4 shows a flow chart containing the basic steps followed for the experimental  $\theta$  measurements.

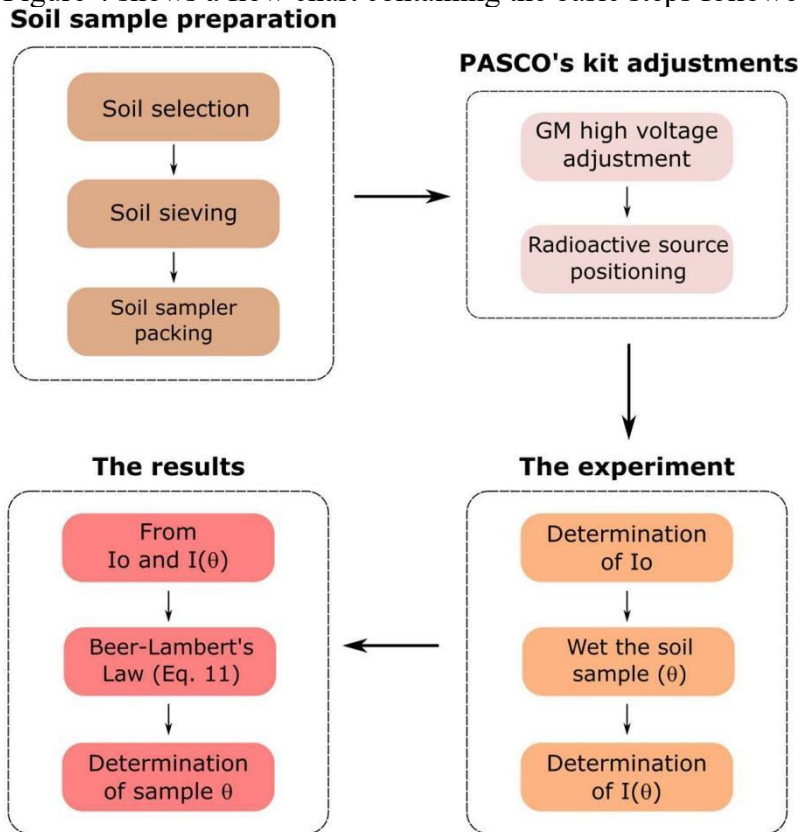


Figure 4. Flow chart of the steps followed for the soil water content ( $\theta$ ) measurement using the simplified gamma-ray attenuation method. GM: Geiger-Müller detector.  $I_0$ : Intensity of the incident photon beam.  $I$ : Intensity of the transmitted photon beam.

#### 4. Results and Discussion

The graphs of the number of photons transmitted ( $I$ ) as a function of the  $\theta$  of the samples showed a linear behavior ( $R$  ranging from  $-0.95$  to  $-0.98$ ) for all the soil types studied (Figure 5). The higher count values observed for HeCa and SiLo were due to the longer counting time adopted for these particular soil samples.

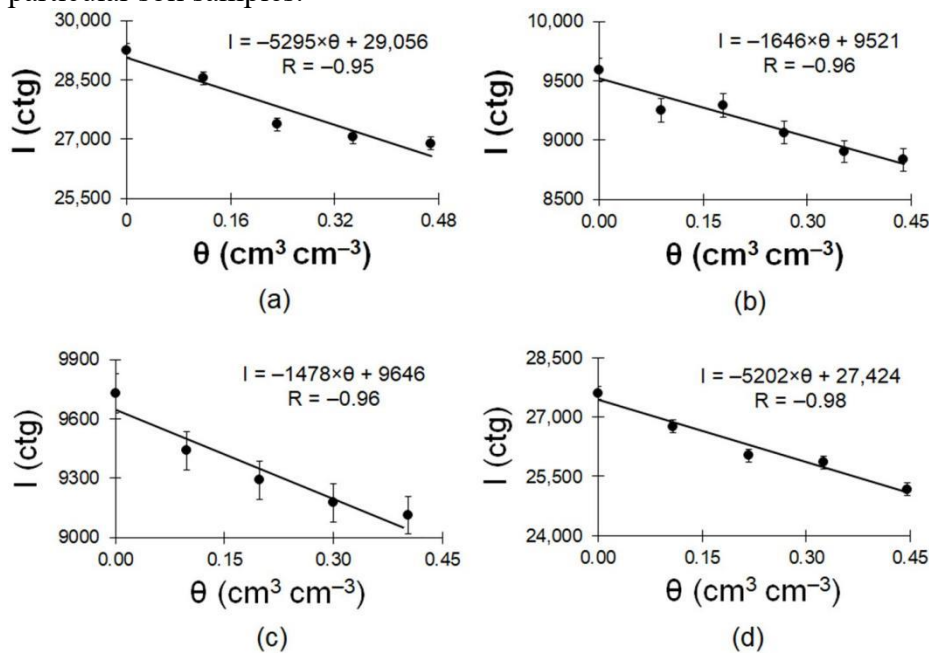


Figure 5. Transmitted gamma-ray photons (I) as a function of the volumetric water content ( $\theta$ ) for the soils: (a) Heavy Clay (HeCa), (b) Clay (Cla), (c) Sandy Clay Loam (SaCLO), and (d) Silt Loam (SiLo). The error bars represent the counting (ctg) statistics.  $\theta$  was kept constant for each counting step.

The differences in the photon counts observed for the dry soil samples ( $\theta = 0 \text{ cm}^3 \text{ cm}^{-3}$ ) are associated with the differences in their compositions. For example, the soil's chemical composition (mainly due to oxide content) and mineralogy will influence the soil properties, such as the particle density, which are directly related to the radiation attenuation (Equation (2)). Another parameter also affected by the soil's chemical composition is the attenuation coefficient [21–23]. For low-energy photons ( $<100 \text{ keV}$ ), the attenuation coefficient is influenced mainly by the photoelectric effect, whose cross-section is proportional to  $Z^4-5$  and inversely proportional to the photon energy ( $E^{-3}$  when  $<500 \text{ keV}$ ) [24,25]. For the intermediate energy region c.  $100 \text{ keV}$  to c.  $10 \text{ MeV}$ , the incoherent scattering influences the photon interaction and, consequently, the attenuation coefficient, whose cross-section has a  $Z$  dependence [26,27]. For high-energy photons ( $E > 10 \text{ MeV}$ ), pair production is the most important process in the attenuation of the radiation associated with the  $Z^2$  dependence of its cross-section. In our study, incoherent scattering was the main process influencing the photon ( $^{137}\text{Cs}$ ) interaction and the attenuation coefficient. For example, Camargo et al. [26], working with tropical/subtropical soils with contrasting major oxide ( $\text{SiO}_2$ ,  $\text{Al}_2\text{O}_3$ ,  $\text{Fe}_2\text{O}_3$ ,  $\text{TiO}_2$ ) compositions, demonstrated that for the photon energy of  $^{137}\text{Cs}$ , the total attenuation coefficient is completely influenced by the incoherent scattering ( $>99\%$ ). Furthermore, these authors mainly associated the dominance of each one of the partial effects (photoelectric effect, incoherent scattering, and pair production) with the  $Z$  dependence on the partial cross-sections, as discussed earlier.

The equations obtained when fitting the experimental data (Figure 5) make it possible to predict  $\theta$  (interpolation) only by knowing the photons transmitted by the sample. However, two precautions for this interpolation are necessary: the sample water volume should not exceed the maximum volume necessary for the saturation of the sample, and for each soil type, a proper calibration equation must be determined. From the  $\theta$  values obtained at saturation, we calculated the total porosity of the analyzed soils by the simplified GRA method using Equation (11) (Table 2). We found total porosity deviations from c.  $7.8\%$  (SiLo) to c.  $18.2\%$  (SaCLO) when compared to the traditional method (Equation (9)).

Table 2. Total porosity ( $\phi$ ) obtained by the traditional (TRA) and simplified gamma-ray attenuation (GRA) methods.

Soil/Methods	TRA	GRA
	$\theta \text{ (cm}^3 \text{ cm}^{-3}\text{)}$	
HeCa	0.591	0.515
Cla	0.445	0.377
SaCLO	0.505	0.413
SiLo	0.540	0.582

HeCa: Heavy Clay; Cla: Clay; SaCLO: Sandy Clay Loam; SiLo: Silt Loam. The traditional soil total porosity was determined through Equation (9), while the porosity based on the radiation attenuation was determined using Equation (11).

The characteristics of each soil and the presence of entrapped air bubbles during the saturation process could affect the obtained results of the total porosity. Thus, assuming  $\theta$  at saturation as the total porosity should be used cautiously. Another reason for the observed discrepancies is that the radioactive source's experimental apparatus is not collimated and there is not a single-channel analyzer to select the photopeak region related to the Caesium- emitted photons. Therefore, both scattered and transmitted photons are detected by the GM detector [27,28]. This fact causes drawbacks in using Equation (11), which should have a correction parameter (buildup factor), which was not covered in our study [29,30] to maintain the analysis as simple as possible.

When we analyze the results of the total porosity (Table 2—traditional method) concerning the particles of the soils (Figure 3), we observe that, in general, higher total porosi- ties are observed in

soils with a larger clay content (HeCa). On the other hand, the predominance of sand particles (SaCLo) causes the total porosity to decrease. Soils with a higher sand content tend to be denser and, consequently, less porous (low porosities), in opposition to clayey soils [1,4]. Thus, our results seem to be consistent with what is expected. Finally, the silt content exerts an intermediate (between clay and sand) influence on this particular soil property.

The comparison of the  $\theta$  values obtained by the traditional and simplified GRA methods shows that, except for HeCa ( $R = 0.90$ ), there was an adequate agreement between the results (Figure 6). The best results were observed for Clay and Silt Loam soils, where the determinations were closer to the 1:1 line. Some reasons can explain the observed differences between the methods. One of them is the simplicity of the electronic system (i.e., no channel analyzer) used to detect the gamma-rays by the nuclear method, i.e., the PASCO kit is designed primarily for teaching purposes, which makes it simpler and more limited compared to those employed in applied nuclear physics research [18]. For example, scattered photons can be detected by the simplified GRA system; this is something that is minimized in systems in which the photon energy to be analyzed can be chosen. Furthermore, the detection and counting of scattered photons limit the use of Equation (11), as mentioned before. Finally, the type of detector utilized (GM) is based on the gas ionization mechanism, which has a lower efficiency in detecting gamma-ray photons of higher energies when compared, for instance, to solid scintillation detectors that are usually employed in research systems [31].

We have to emphasize that although numerous other techniques are used in  $\theta$  monitoring, the technique based on gamma-ray attenuation is well established and employed to this day [12,32–36]. This nuclear method enables fast (for high-activity radioactive sources) and accurate measurements of  $\theta$  [20]. Furthermore, this versatile method allows measurements under field and laboratory conditions [32,33]. Our study proposed applying the simplified nuclear system in laboratory measurements of  $\theta$ , utilizing disturbed soil samples with small volumes as a didactic activity. These samples were idealized considering the limitations of the Intermediate Nuclear Laboratory System [17], such as the low activity of the radioactive source (radiological protection issue for teaching activities), the type and size of the detector used, and the dimensions of the sample holder. Nonetheless, our study's core idea was to show that even the simplified GRA system gives satisfactory results and might be employed to explore concepts related to the technique itself (physical principles) and the principles of operation of the electronics and gamma-ray detector.

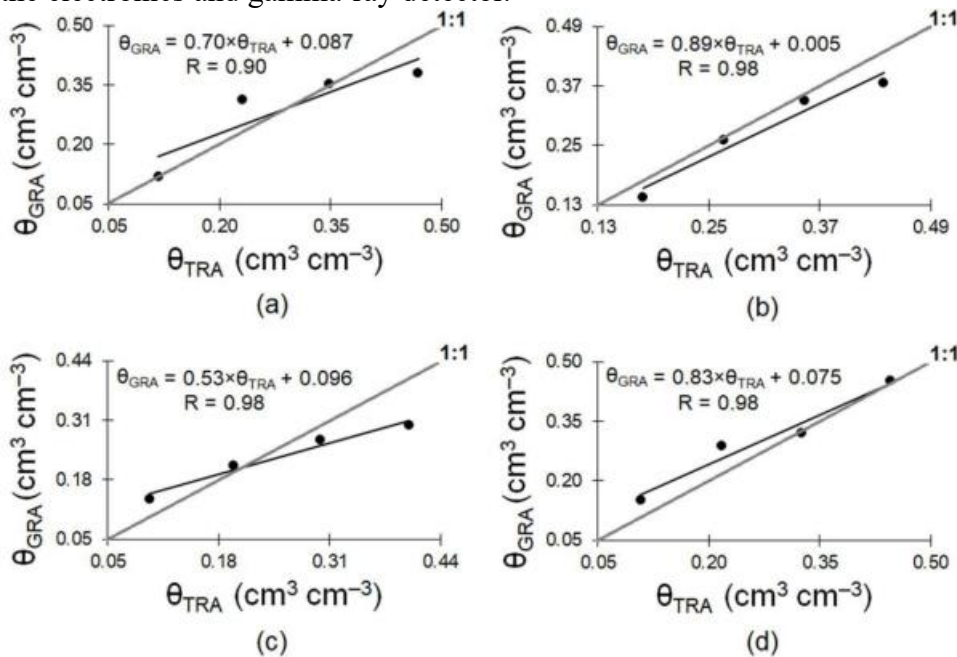


Figure 6. Comparison of the soil water content ( $\theta$ ) evaluated by the traditional ( $\theta_{TRA}$ —Equation (4)) and simplified gamma-ray attenuation ( $\theta_{GRA}$ —Equation (11)) methods (1:1 line) for the contrasting soils: (a) Heavy Clay (HeCa), (b) Clay (Cla), (c) Sandy Clay Loam (SaCLo), and (d) Silt Loam (SiLo).



The error bars for  $\theta$ GRA are not presented in the graphs due to their magnitudes (varied from 0.0002 to 0.0016 cm<sup>3</sup> cm<sup>-3</sup>).  $\theta$ TRA was kept constant during the experimental procedure.

## 5. Conclusions

The current investigation demonstrated the viability of a streamlined gamma-ray attenuation apparatus to determine  $\theta$ . Furthermore, by using the Beer-Lambert formula to calculate  $\theta$  at saturation, we were able to assess the overall porosity of the samples. When compared to the conventional radiation attenuation-based methods, the nuclear method for  $\theta$  monitoring was much more constrained and had a distinct setup. As previously mentioned, for the measurements, we used a non-collimated system, low-activity radioactive sources, a gas-filled (GM) tube detector, and simple electronics. Thus, the limits of the reduced nuclear system may be the primary reason for the disparities between the GRA technique and the usual way of  $\theta$  evaluation. Nevertheless, in spite of these drawbacks, we were nevertheless able to ascertain  $\theta$  and the overall porosity of soil samples with differing textural fractions using the nuclear approach that was described. The need for distinct calibrations for  $\theta$  estimation based on nuclear methods can be explained by changes in the composition of the soil (grain sizes and chemical composition). However, the process of calibration can be viewed as a preliminary educational exercise that demonstrates how fluctuations in the photon counts are related to changes in the composition of the soil. Additionally, we stated that in order to raise the method's intrinsic sensitivity connected to the GRA approach, the counting time needs to be improved. We propose employing radioactive sources (such as <sup>133</sup>Ba or <sup>241</sup>Am) that release less energetic gamma-ray photons and collimating the photon beam before it reaches the GM tube as future improvements. Overall, our results showed that undergraduate students may find the simplified nuclear system and methodology to be an engaging tool for teaching them about radiation detection, nuclear electronics, gamma-ray attenuation, and the examination of specific soil properties.

**Additional Resources:** You can obtain the supporting data at <https://www.mdpi.com/article/10.3390/agriengineering5020068/s1>. Figure S1. An image of the experimental setup used to measure the moisture content of the soil. Table S1 lists the parameters used to measure the water content of soil using the gamma-ray attenuation method. Table S2. Gravimetric water content (G) measured using the gamma-ray attenuation method during experimental soil moisture measurements. Table S3. Analysis of the different gravimetric soil water content (G) values. Transmitted beam intensity (I).

**Contributions of the Author:** Writing—original draft preparation: L.F.P. and F.A.M.C.; conceptualization: L.F.P. and F.A.M.C.; methodology: L.F.P. and F.A.M.C.; formal analysis: L.F.P. and F.A.M.C.; investigation: L.F.P. and F.A.M.C. After reading the published version of the manuscript, each author gave their approval. After reading the published version of the manuscript, all writers have given their approval.

**support:** There was no outside support for this study.

**Data Availability Statement:** Upon reasonable request to [lfpires@uepg.br](mailto:lfpires@uepg.br), all data are available.

**Conflicts of Interest:** None that the writers are aware of exist.

## References

1. Hillel, D. *Environmental Soil Physics*; Academic Press: San Diego, CA, USA, 1998.
2. Pimentel, D.; Berger, B.; Filiberto, D.; Newton, M.; Wolfe, B.; Karabinakis, E.; Clark, S.; Poon, E.; Abbett, E.; Nandagopal, S. *Water Resources: Agricultural and Environmental Issues*. *BioScience* 2004, 54, 909–918. [CrossRef]
3. Tarawally, M.A.; Medina, H.; Frómeta, M.E.; Alberto Itza, C. Field Compaction at Different Soil-Water Status: Effects on Pore Size Distribution and Soil Water Characteristics of a Rhodic Ferralsol in Western Cuba. *Soil Tillage Res.* 2004, 76, 95–103. [CrossRef]
4. Lal, R.; Shukla, M.K. *Principles of Soil Physics*; Marcel Dekker, Inc.: New York, NY, USA, 2004.
5. Reichardt, K.; Timm, L.C. *Soil, Plant and Atmosphere: Concepts, Processes and Applications*; Springer Nature: Cham, Switzerland, 2020.

6. Pires, L.F.; Cássaro, F.A.M.; Correchel, V. Use of Nuclear Techniques in Soil Science: A Literature Review of the Brazilian Contribution. *Rev. Bras. Ci. Solo* 2021, 45, e0210089. [CrossRef]
7. Wang, J.; Watts, D.B.; Meng, Q.; Ma, F.; Zhang, Q.; Zhang, P.; Way, T.R. Influence of Soil Wetting and Drying Cycles on Soil Detachment. *AgriEngineering* 2022, 4, 533–543. [CrossRef]
8. Dapla, P.; Hriník, D.; Hrabovský, A.; Simkovic, I.; Zarnovican, H.; Sekucia, F.; Kollár, J. The Impact of Land-Use on the Hierarchical Pore Size Distribution and Water Retention Properties in Loamy Soils. *Water* 2020, 12, 339.
9. Buckingham, E. Studies on the Movement of Soil Moisture; Bulletin, No. 38; United States Department of Agriculture, Bureau of Soil: Washington, DC, USA, 1907.
10. Celik, N.; Altin, D.; Cevik, U. A New Approach for Determination of Volumetric Water Content in Soil Samples by Gamma-Ray Transmission. *Water Air Soil Pollut.* 2016, 227, 207. [CrossRef]
11. Schaap, M.G.; Leij, F.J. Using Neural Networks to Predict Soil Water Retention and Soil Hydraulic Conductivity. *Soil Tillage Res.* 1998, 47, 37–42. [CrossRef]
12. Demir, D.; Ün, A.; Özgül, M.; Sahin, Y. Determination of Photon Attenuation Coefficient, Porosity and Field Capacity of Soil by Gamma-Ray Transmission for 60, 356 and 662 keV Gamma Rays. *Appl Radiat Isot.* 2008, 66, 1834–1837. [CrossRef]
13. Filiz Baytas, A.; Akbal, S. Determination of Soil Parameters by Gamma-Ray Transmission. *Radiat Meas.* 2002, 35, 17–21. [CrossRef]
14. Oliveira, J.C.M.; Appoloni, C.R.; Coimbra, M.M.; Reichardt, K.; Bacchi, O.O.S.; Ferraz, E.; Silva, S.C.; Galvão Filho, W. Soil Structure Evaluated by Gamma-Ray Attenuation. *Soil Tillage Res.* 1998, 48, 127–133. [CrossRef]
15. Naime, J.M.; Vaz, C.M.P.; Macedo, A. Automated Soil Particle Size Analyzer based on Gamma-Ray Attenuation. *Comput. Electron. Agric.* 2001, 31, 295–304. [CrossRef]
16. Elsafi, M.; Koraim, Y.; Almurayshid, M.; Almasoud, F.I.; Sayyed, M.I.; Saleh, I.H. Investigation of Photon Radiation Attenuation Capability of Different Clay Materials. *Materials* 2021, 14, 6702. [CrossRef]
17. PASCO. Available online: <https://www.pasco.com/products/lab-apparatus/atomic-and-nuclear/sn-7900#desc-panel> (accessed on 23 March 2023).
18. Pires, L.F.; Cássaro, F.A.M.; Tech, L.; Pereira, L.A.A.; de Oliveira, J.A.T. Gamma Ray Attenuation for Determining Soil Density: Laboratory Experiments for Environmental Physics and Engineering Courses. *Rev. Bras. Ens. Fis.* 2020, 42, e20190340. [CrossRef]
19. Amoozegar, A.; Heitman, J.L.; Kranz, C.N. Comparison of soil particle density determined by a gas pycnometer using helium, nitrogen, and air. *Soil Sci. Soc. Am. J.* 2023, 87, 1–12. [CrossRef]
20. Ferraz, E.S.B.; Mansell, R.S. Determining Water Content and Bulk Density of Soil by Gamma-Ray Attenuation Methods; Technical Bulletin No. 807; University of Florida: Gainesville, FL, USA, 1979.
21. Al-Masri, M.S.; Hasan, M.; Al-Hamwi, A.; Amin, Y.; Doubal, A.W. Mass Attenuation Coefficients of Soil and Sediment Samples using Gamma Energies from 46.5 to 1332 keV. *J. Environ. Radioact.* 2013, 116, 28–33. [CrossRef] [PubMed]
22. Cesareo, R.; Assis, J.T.; Crestana, S. Attenuation Coefficients and Tomographic Measurements for Soil in the Energy Range 10–300 keV. *Appl. Radiat. Isot.* 1994, 45, 613–620. [CrossRef]
23. Bhandal, G.S.; Singh, K. Photon Attenuation Coefficient and Effective Atomic Number Study of Cements. *Appl. Radiat. Isot.* 1993, 44, 1231–1243. [CrossRef]
24. Appoloni, C.R.; Rios, E.A. Mass Attenuation Coefficients of Brazilian Soils in the Range 10–1450 keV. *Appl. Radiat. Isot.* 1994, 45, 287–291. [CrossRef]
25. Kaplan, I. Nuclear Physics; Addison-Wesley Publishing Company: Cambridge, UK, 1963.
26. Camargo, M.A.; Kodum, K.S.; Pires, L.F. How Does the Soil Chemical Composition Affect the Mass Attenuation Coefficient? A Study Using Computer Simulation to Understand the Radiation-Soil Interaction Processes. *Braz. J. Phys.* 2021, 51, 1775–1783. [CrossRef]
27. Knoll, G.F. Radiation Detection and Measurement; John Wiley & Sons, Inc.: Hoboken, NJ, USA, 2010.

28. Abdel-Rahman, M.A.; Badawi, E.A.; Abdel-Hady, Y.L.; Kamel, N. Effect of Sample Thickness on the Measured Mass Attenuation Coefficients of Some Compounds and Elements for 59.54, 661.6 and 1332.5 keV  $\gamma$ -rays. Nucl. Instrum. Methods Phys. Res. A 2000, 447, 432–436. [CrossRef]
29. Sharaf, J.M.; Saleh, H. Gamma-Ray Energy Buildup Factor Calculations and Shielding Effects of Some Jordanian Building Structures. Radiat. Phys. Chem. 2015, 110, 87–95. [CrossRef]
30. Brar, G.S.; Sidhu, G.S.; Sandhu, P.S.; Mudahar, G.S. Variation of Buildup Factors of Soils with Weight Fractions of Iron and Silicon. Appl. Radiat. Isot. 1998, 49, 977–980. [CrossRef]
31. Wang, C.H.; Willis, D.L.; Loveland, W.D. Radiotracer Methodology in the Biological, Environmental, and Physical Sciences; Prentice-Hall, Inc.: New Jersey, NJ, USA, 1975.
32. Ferguson, H.; Gardner, W.H. Water Content Measurement in Soil Columns by Gamma Ray Absorption. Soil Sci. Soc. Proceed. 1962, 26, 11–14. [CrossRef]
33. Reginato, R.J.; van Bavel, C.H.M. Soil Water Measurement with Gamma Attenuation. Soil Sci. Soc. Am. Proceed. 1964, 28, 721–724. [CrossRef]
34. Moreno-Barbero, E.; Kim, Y.; Saenton, S.; Illangasekare, T.H. Intermediate-Scale Investigation of Nonaqueous-Phase Liquid Architecture on Partitioning Tracer Test Performance. Vadose Zone J. 2007, 6, 725–734. [CrossRef]
35. Bacchi, O.O.S.; Reichardt, K.; Oliveira, J.C.M.; Nielsen, D.R. Gamma-Ray Beam Attenuation as an Auxiliary Technique for the Evaluation of Soil Water Retention Curve. Sci. Agric. 1998, 55, 499–502. [CrossRef]
36. Medhat, M.E. Application of Gamma-Ray Transmission Method for Study the Properties of Cultivated Soil. Ann. Nucl. Energy 2012, 40, 53–59. [CrossRef]